Inorganic Chemistry

Article

pubs.acs.org/IC

Synthesis and Characterization of the Titanium Bisamide Ti{N(H)Ar^{iPr_6}}$_2$ (Ar^{iPr_6} = C$_6$H$_3$-2,6-(C$_6$H$_2$-2,4,6-^{i}Pr$_3$)$_2$ and Its TiCl{N(H)Ar^{iPr_6}}$_2$ Precursor: Ti(II) → Ti(IV) Cyclization

Jessica N. Boynton,[†] Jing-Dong Guo,[‡] Fernande Grandjean,[§] James C. Fettinger,[†] Shigeru Nagase,[‡] Gary J. Long,[§] and Philip P. Power*[,†]

[†]Department of Chemistry, University of California, Davis, California 95616, United States

[‡]Fukui Institute for Fundamental Chemistry, Kyoto University, 34-4 Takano-Nishihiraki-cho, Sakyou-ku, Kyoto 606−8103, Japan

[§]Department of Chemistry, Missouri University of Science and Technology, University of Missouri, Rolla, Missouri 65409-0010, United States

Supporting Information

ABSTRACT: The titanium bisamido complex Ti{N(H)Ar^{iPr_6}}$_2$ (Ar^{iPr_6} = C$_6$H$_3$-2,6-(C$_6$H$_2$-2,4,6-^{i}Pr$_3$)$_2$ (**2**), along with its three-coordinate titanium(III) precursor, TiCl{N(H)Ar^{iPr_6}}$_2$ (**1**), have been synthesized and characterized. Compound **1** was obtained via the stoichiometric reaction of LiN(H)Ar^{iPr_6} with the Ti(III) complex TiCl$_3$·2NMe$_3$ in trimethylamine. Reduction of **1** with 1 equiv of KC$_8$ afforded Ti{N(H)Ar^{iPr_6}}$_2$ (**2**) in moderate yield. Both **1** and **2** were characterized by X-ray crystallography, NMR, and IR spectroscopy, magnetic studies, and by density functional theory (DFT) computations. The precursor **1** has quasi-four-coordinate coordination at the titanium atom, with bonding to two amido nitrogens and a chlorine as well as a secondary interaction to a flanking aryl ring of a terphenyl substituent. Compound **2** displays a very distorted four-coordinate metal environment in which the titanium atom is bound to two amido nitrogens and to two carbons from a terphenyl aryl ring. This structure is in sharp contrast to the expected two-coordinate linear structure that was observed in its first row metal (V−Ni) analogues. Magnetic studies confirm a d^1 electron configuration for **1** but indicate that Ti{N(H)Ar^{iPr_6}}$_2$ (**2**) is diamagnetic at ambient temperature consistent with the oxidation of titanium to Ti(IV). The different structure of **2** is attributed to the high reducing tendency of the Ti(II) in comparison to the other metals.

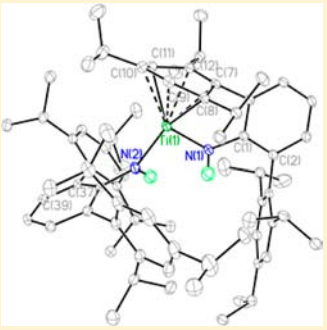

INTRODUCTION

The use of sterically demanding amido ligands has allowed the isolation and characterization of several rare, open-shell (d^1-d^9 electron configuration) two-coordinate transition metal complexes.[1,2] Such complexes are of interest for several reasons which include an increased number of open sites for the coordination of small molecules, low-numbers of electrons in the metal valence shell as well as their magnetic properties. The latter are of interest because the low number of ligands tends to minimize the quenching of orbital angular momentum (OAM) especially when the geometry of the complex is linear.[3−10] Currently, linear coordination in the solid state is limited to about a dozen open-shell complexes.[1,4−8,10−12] Moreover their electron counts are, with one exception,[12] confined to those with d^4-d^8 electron configurations. Recently, it has been shown that the use of the bulky amido ligand −N(H)Ar^{iPr_6} (Ar^{iPr_6} = C$_6$H$_3$-2,6-(C$_6$H$_2$-2,4,6-^{i}Pr$_3$)$_2$ could stabilize the d^3 complex V{N(H)Ar^{iPr_6}}$_2$ which had a linear metal coordination and magnetic properties consistent with the presence of significant OAM.[12] This was the first example of a crystalline two-coordinate vanadium complex and in addition the first homoleptic V(II) amido derivative. We resolved to extend the use of the large −N(H)Ar^{iPr_6} ligand to titanium with the object of synthesizing its d^2, titanium(II) analogue Ti{N(H)Ar^{iPr_6}}$_2$.

We now describe the synthesis, characterization, and magnetic properties of Ti{N(H)Ar^{iPr_6}}$_2$ (**2**) and its precursor TiCl{N(H)Ar^{iPr_6}}$_2$ (**1**). The latter species features a quasi-four-coordinate geometry for the Ti^{3+} ion and displays magnetic properties consistent with a d^1 electron configuration. However, in contrast to other first row metal derivatives it is shown that the nominally two-coordinate, Ti(II) bisamido complex Ti{N(H)Ar^{iPr_6}}$_2$ (**2**) undergoes an addition reaction with a flanking aryl ring of a terphenyl substituent to a produce a cyclized Ti(IV) product.

EXPERIMENTAL SECTION

General Procedures. All manipulations were carried out under anaerobic and anhydrous conditions by using modified Schlenk line techniques under a dinitrogen atmosphere or in a Vacuum Atmospheres HE-43 drybox. All of the solvents were first dried by the method of Grubbs et al. and then stored over potassium.[13] All physical measurements were obtained under strictly anaerobic and anhydrous

Received: August 20, 2013
Published: November 22, 2013

   dx.doi.org/10.1021/ic4021355 | Inorg. Chem. 2013, 52, 14216−14223

Table 1. Selected Crystallographic and Data Collection Parameters for Titanium Complexes 1 and 2

compound	$TiCl\{N(H)Ar^{iPr_6}\}_2\cdot(n\text{-}C_6H_{14})_2$ (**1**·2 hexane)	$Ti\{N(H)Ar^{iPr_6}\}_2$ (**2**)
empirical formula	$C_{84}H_{128}ClN_2Ti$	$C_{72}H_{100}N_2Ti$
formula weight (g/mol)	1249.21	1041.43
crystal system	triclinic	triclinic
space group	$P\bar{1}$	$P\bar{1}$
a (Å)	14.7300(5)	12.8989(15)
b (Å)	15.2643(5)	13.5582(16)
c (Å)	19.6629(6)	20.951(2)
α (deg)	87.7219(5)	76.306(5)
β (deg)	72.4363(4)	88.769(5)
γ (deg)	65.1037(4)	63.044(5)
volume (Å^3)	3803.8(2)	3157.4(7)
Z	2	2
density (calculated) (Mg/m^3)	1.089	1.095
absorption coefficient (mm^{-1})	0.190	1.443
F(000)	1366	1136
crystal size (mm)	0.282 × 0.237 × 0.161	0.549 × 0.372 × 0.266
crystal color and habit	orange, prism	dark orange, trapezoid
θ range for data collection	2.167 to 27.481°	7.137 to 68.164°
reflections collected	34082	16327
independent reflections	17383 [R(int) = 0.0267]	10878 [R(int) = 0.0324]
observed reflections ($I > 2\sigma(I)$)	13601	9703
data/restraints/parameters	17383/35/851	10878/7/771
goodness-of-fit on F^2	1.032	1.016
final R indices [$I > 2\sigma(I)$]	R1 = 0.0480, wR2 = 0.1234	R1 = 0.0584, wR2 = 0.1565
R indices (all data)	R1 = 0.0644, wR2 = 0.1347	R1 = 0.0638, wR2 = 0.1613

conditions. IR spectra were recorded as Nujol mulls between CsI plates on a Perkin-Elmer 1430 Infrared Spectrometer. UV−visible spectra were recorded as dilute hexane solutions in 3.5 mL quartz cuvettes using a HP 8452 diode array spectrophotometer. Melting points were determined on a Meltemp II apparatus using glass capillaries sealed with vacuum grease, and are uncorrected. Unless otherwise stated, all materials were obtained from commercial sources and used as received. $LiN(H)Ar^{iPr_6}$ was prepared according to literature procedures.[14] KC_8[15] was prepared by heating a 8:1 mixture of graphite to potassium until a copper color was achieved, and stored under an inert atmosphere.

$TiCl\{N(H)Ar^{iPr_6}\}_2$ (1). Trimethylamine (ca. 50 mL) was added to $TiCl_3$ (1.00 g, 6.48 mmol) at about −78 °C and stirred for 1 week at this temperature.[15] To the resulting turquoise/gray slurry 5.98 g of $LiN(H)Ar^{iPr_6}$ (11.9 mmol) was added via a solids addition funnel. The resulting mixture was allowed to stir at about −78 °C for about 3 days. The flask was allowed to warm to room temperature, and NMe_3 was removed under reduced pressure. The resulting red-orange solid was extracted with hexane (ca. 25 mL) and filtered via cannula. The red-orange solution was concentrated to about 20 mL and, upon storage for about 1 week at about −18 °C, afforded X-ray quality orange crystals of **1**. Yield 4.12 g (64%), mp 134−137 °C. UV−vis, nm (ε, M^{-1} cm^{-1}), 11,000 (298), 4200 (356), and 2700 (415). IR in Nujol mull (cm^{-1}) in KBr: ν_{N-H} 3467, 3368(w).

$Ti\{N(H)Ar^{iPr_6}\}_2$ (2). To a powdered mixture of KC_8 (0.015 g, 0.110 mmol) and 0.111 g of **1** (0.103 mmol) about 30 mL of pentane was added dropwise over about 30 min at about 0 °C . An immediate darkening of the solution from a red-orange to a dark brown color was observed. The solution was allowed to warm to room temperature and was stirred for about 4 days. The resulting KCl and graphite precipitate was filtered off via cannula, and the resulting orange brown solution was concentrated to about 5 mL. Storage for about 3 days in pentane at about 25 °C afforded X-ray quality dark orange plates. Yield 0.048 g (46%), mp 160−162 °C. UV−vis, nm (ε, M^{-1} cm^{-1}), 10,000 (293), 5500 (363), and 2400 (451). IR in Nujol mull (cm^{-1}) in KBr: ν_{N-H} 3465, 3367(w). ^{1}H NMR (500 MHz, C_6D_6, 303 K): 1.14 (d, 24H), 1.21 (d, 24H), 1.26 (d, 24H), 1.37 (d, 6H), 1.41 (d, 3H), 2.87 (sep, 2H), 2.97 (s, 2H), 3.03 (sep, 4H), 6.48 (b, 2H), 6.87 (b, 6H), 7.00 (s, 1H), 7.03 (d, 2H), 7.23 (s, 2H), 7.25(s, 4H), 7.28 (s, 1H), 7.32 (s, 2H). ^{13}C NMR (100.6 MHz, C_7D_8, 298 K): δ 24.8, 25.2, 31.3, 35.3, 118.1, 121.8, 129.9, 134.2, 137.7, 143.3, 148.4, 149.1.

X-ray Crystallography. Bright orange and dark orange X-ray quality crystals of **1** and **2**, respectively, were obtained from concentrated pentane solutions after storage at about −18 °C for 1 week (**1**) or at about 25 °C for 3 days (**2**). Suitable crystals were selected and covered with a layer of hydrocarbon oil under a rapid flow of dinitrogen. They were mounted on a glass fiber attached to a copper pin and placed in a cold N_2 stream on a diffractometer.[17] X-ray data for **1** were collected at 90(2) K with (λ = 0.71073 Å) Mo Kα radiation with the Bruker SMART Apex II diffractometer. Data for **2** were collected at 90(2) K with (λ = 1.5418 Å) Cu Kα_1 radiation using a Bruker DUO diffractometer in conjunction with a CCD detector. The collected reflections were corrected for Lorentz and polarization effects and for absorption by use of Blessing's method as incorporated into the program SADABS.[18a] The structures were solved by direct methods and refined with the SHELXTL v.6.1 software package.[18b] Refinement was by full-matrix least-squares procedures with all carbon-bound hydrogen atoms included in calculated positions and treated as riding atoms. N-bound hydrogens were located directly from the Fourier difference map. A summary of crystallographic and data collection parameters for **1** and **2** are given in Table 1.

Magnetic Measurements. Powdered samples of **1** and **2** were sealed under vacuum in 5 mm diameter quartz tubes. The magnetic properties were measured using a Quantum Design MPMSXL7 superconducting quantum interference magnetometer; the samples were first zero-field cooled to 2 K, and their moments were measured upon warming from 2 to 300 K in an applied field of 0.01 T. To ensure thermal equilibrium between the sample in the quartz tube and the temperature sensor, the moment was measured at each temperature until it reached a constant value; about 15 h were required for the measurements. Diamagnetic corrections of −0.000792 emu/mol and −0.000769 emu/mol, obtained from tables of Pascal's constants,[19] were applied respectively to the measured molar magnetic susceptibility of **1**

dx.doi.org/10.1021/ic4021355 | Inorg. Chem. 2013, 52, 14216−14223

Scheme 1. Synthetic Routes to TiCl{N(H)Ar^{iPr_6}}$_2$ (1) and Ti{N(H)Ar^{iPr_6}}$_2$ (2)

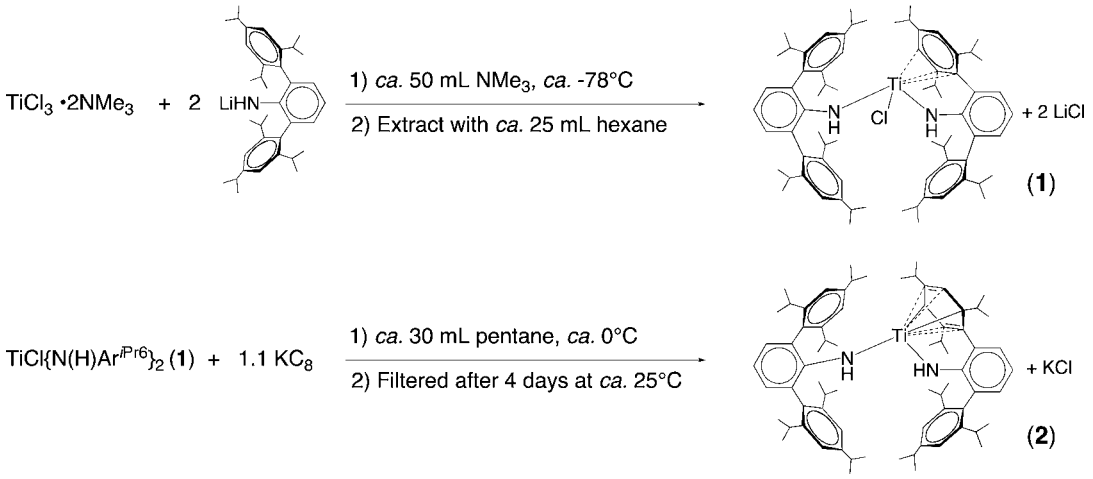

and **2**. Following the above study, the same sample was cooled to 5 K, and its magnetization was measured in a field of ±5 T; no magnetic hysteresis was observed in this study.

Density Functional Theory. All calculations were carried out using the Gaussian 09 program.[20] Geometry optimization was performed with hybrid density functional theory (DFT) at the unrestricted B3PW91[21] level. Based on the optimized geometries, the unscaled vibrational frequencies and the UV/vis absorption wavelengths estimated by the time dependent DFT (TD-DFT) method were obtained with the UB3PW91 wave function.

RESULTS AND DISCUSSION

Synthesis. Compound **1** was synthesized via a salt metathesis route (Scheme 1) by the reaction of the Lewis base complex $TiCl_3{\cdot}2NMe_3$[22] with LiN(H)Ar^{iPr_6}[14] in a 1:2 ratio in trimethylamine, which gave moderate, reproducible yields of TiCl{N(H)Ar^{iPr_6}}$_2$ (**1**). Initial experiments involving the reaction of the lithium amide with the more readily available Ti(III) halide precursor $TiCl_3(THF)_3$[23] as the titanium source were unsuccessful. Compound **2** was synthesized via the reduction of compound **1** with a slightly greater than stoichiometric amount of potassium graphite. Attempts to use a gentler reducing agent (Na) to increase yield were unsuccessful. We found that unlike many titanium(II) complexes which are known to bind to dinitrogen,[24] the reduction of **1**, although performed under N_2, showed no evidence of reaction with the N_2 atmosphere.

Structures. The structure of **1** is shown in Figure 1, and selected bond distances and angles are given in Table 2. The complex TiCl{N(H)Ar^{iPr_6}}$_2$ (**1**) exists as well separated monomers in which a slipped piano stool geometry at the titanium atom is bound to two amido nitrogens and a chlorine atom. The N(1)−Ti(1)−N(2) angle (132.08(0)°) is the widest of the interligand angles at the titanium atom as a result of steric repulsion between the terphenyl amido groups. In addition, there is an interaction between titanium and a flanking ring of one of the terphenyl substituents such that the Ti(1)−N(1)−N(2)−Cl(1) array becomes nonplanar Σ°Ti = 343.35(6)°. The Ti−C bond distances to the carbons of the interacting aryl ring are in the range of ca. 2.49−2.69 Å and are longer than those observed in titanocene or for other titanium aryl interactions which range from 2.2 to 2.4 Å.[25,26] The shortest Ti−C distance to the flanking aryl ring (Ti−C(8)= 2.4854(16) Å) is considerably longer than about 2.11 Å that would be expected for a Ti(III)−C single bond.[27] There is a considerable difference (ca. 22.4°) between the two Ti(1)−N−C(ipso) angles with the narrower angle associated with the amido ligand involving the Ti-flanking ring interaction at N(1). The Ti(1)−N(1) bond distance

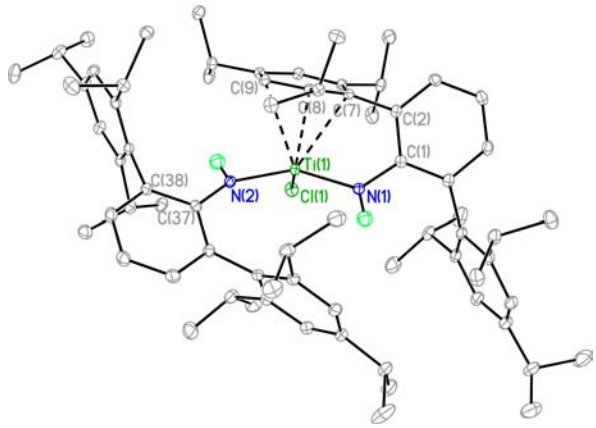

Figure 1. X-ray crystal structure of the three-coordinate TiCl{N(H)Ar^{iPr_6}}$_2$ (**1**). (Non-nitrogen H atoms are not shown for clarity, thermal ellipsoids are shown at 30% probability.) Selected bond distances and angles are given in Table 2

Table 2. Selected Interatomic Distances (Å) and Angles (deg) for the Complexes 1 and 2

	TiCl{N(H)Ar^{iPr_6}}$_2$ (**1**)	Ti{N(H)Ar^{iPr_6}}$_2$ (**2**)
Ti(1)−N(1) Å	1.9901(14)	2.0142(19)
Ti(1)−N(2) Å	1.9532(14)	1.9642(18)
Ti(1)−Cl(1) Å	2.3034(5)	
Ti(1)−C(7) Å	2.6149(16)	2.332(2)
Ti(1)−C(8) Å	2.4854(16)	2.143(2)
Ti(1)−C(9) Å	2.6869(16)	2.399(2)
Ti(1)−C(10) Å	3.101(16)	2.458(3)
Ti(1)−C(11) Å	3.288(16)	2.277(2)
Ti(1)−C(12) Å	3.067(16)	2.434(2)
Ti(1)−centroid	2.524(16)	1.859(2)
N(1)−Ti(1)−N(2) (deg)	132.08(6)	105.56(8)
N(1)−Ti(1)−Cl(1) (deg)	108.24(4)	
N(2)−Ti(1)−Cl(1) (deg)	103.03(5)	
Ti(1)−N(1)/N(2)−(H) (deg)	119.8(15)/98.4(16)	123(2)/97.6(17)
Ti(1)−N(1)−C(1) (deg)	128.70(11)	125.16(15)
Ti(1)−N(2)−C(37) (deg)	151.12(12)	149.31(15)

dx.doi.org/10.1021/ic4021355 | Inorg. Chem. 2013, 52, 14216−14223

Table 3. DFT B3PW91 Calculated Select Bond Distances and Angles for Complexes 1 and 2

	$TiCl\{N(H)Ar^{iPr_6}\}_2$ (1)		$Ti\{N(H)Ar^{iPr_6}\}_2$ (2)	
	calc. B3PW91	experiment	calc. B3PW91	experiment
Ti–N (Å)	1.983/1.954	1.990/1.953	2.011/1.997	2.014/1.964
Ti–Cl (Å)	2.298	2.303		
N–C (Å)	1.398/1.399	1.400/1.394	1.395/1.396	1.405/1.408
N–Ti–N (deg)	132.7	132.1	101.7	105.6
Ti–N–C (deg)	128.9/153.7	128.7/151.1	123.4/154.3	125.2/149.3

(1.9901(14) Å) is also slightly longer than that of Ti(1)–N(2), 1.9532(14) Å. The difference in length is due presumably to changed hybridization as indicated by the Ti(1)–N(1)–C(ipso) angles. These distances are similar to those in other three or four coordinate Ti(III) complexes[24,28] and are consistent with the sum of the single bond radii of (nitrogen + titanium) 2.07 Å.[27] Bond distances and angles predicted by DFT calculations on the full molecule (Table 3) are close to those measured experimentally.

The structure of **2** is shown in Figure 2, and selected bond distances and angles are shown in Table 2. The structure

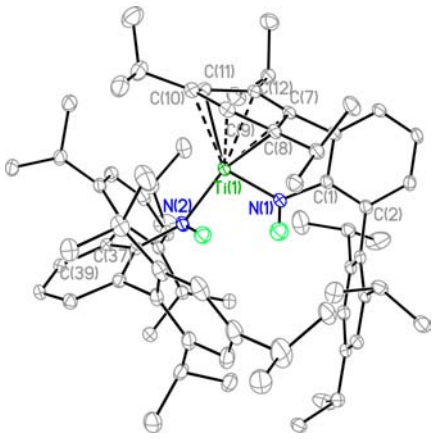

Figure 2. X-ray crystal structure of $Ti\{N(H)Ar^{iPr_6}\}_2$ (**2**). (Non-nitrogen H atoms are not shown for clarity, thermal ellipsoids are shown at 30% probability.) Select bond distances and angles are given in Table 2

confirms the removal of the chlorine from **1** by reduction to form complex $Ti\{N(H)Ar^{iPr_6}\}_2$ (**2**). Although the -$N(H)Ar^{iPr_6}$ ligand has been shown to be effective in stabilizing linear two-coordination in the series $M\{N(H)Ar^{iPr_6}\}_2$ (M = V, Cr, Mn, Fe, Co, and Ni)[5–7,29] this is not the case for titanium. In addition to two bonds to the nitrogens of two amido ligands, the titanium atom is coordinated strongly to one of the flanking aryl rings, causing distortion within the ring which disrupts its aromatic character. The strong Ti-ring interaction also causes severe bending of the geometry of the N(1)–Ti(1)–N(2) array to an angle of 105.56(8)°. Figure 3 provides schematic illustration of the structure of the Ti-aryl moiety where it is apparent that Ti(1) is strongly bound in a 1,4 fashion to the C(8) (2.143(2) Å) and C(11) (2.277(2) Å) atoms of the ring to form, in effect, a cyclohexadienyl moiety bound by two Ti–C σ bonds to the metal with a fold angle of 24.196° along the C(8)–C(11) axis. The titanium thus becomes four-coordinate with a distorted tetrahedral geometry and a +4 oxidation state. The cyclohexadienyl character of the complexed ring is supported by the fact that four of the six C–C ring bonds are lengthened to a range of 1.441(3)–1.497(3) Å consistent with the 1.48 Å predicted for C–C single bonding between sp^2-hybridized carbon atoms.[27a,30]

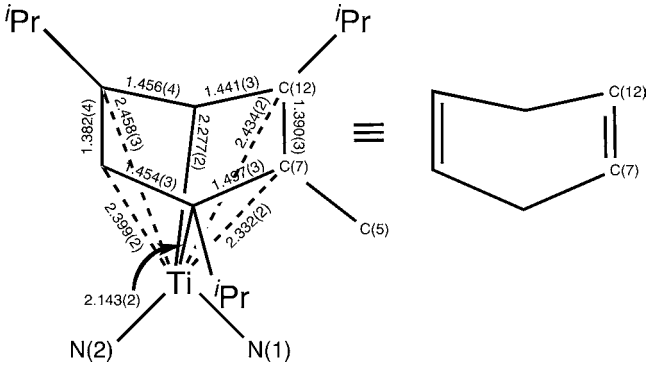

Figure 3. Metrical parameters of the bonding of the C(7)–C(12) ring to the titanium atom in $Ti\{N(H)Ar^{iPr_6}\}_2$ (**2**). All distances are in Å.

In contrast, the C(9)–C(10) and C(7)–C(12) bond lengths retain double character with distances of 1.382(4) and 1.390(3) Å.[27b] The ring bonding distances are displayed in Figure 3. Similar behavior in coordinated aryl rings has been observed by Hagadorn and Arnold in $(L^{Me})Ti(\eta^6\text{-}PhCH_3)$ (L^{Me} = C_6H_4-1,2(NC(*p*-tolyl)NPh)$_2$)[2–31] and Stephan and co-workers in compounds $[Cp_2Ti(NP^tBu_2(2\text{-}C_6H_4Ph))]$.[32] We assume that cyclization occurs in **2** and the other species because of the very low (two) metal electron count and the increased availability of either d or s valence orbitals to participate in a further reaction.

The Ti–N bond-lengths are marginally longer than those in compound **1** despite the increase in oxidation state from titanium(II) to titanium(IV), perhaps as a result of the highly crowded metal environment in **2**. However, the Ti–N bond lengths in **2** are similar to those of other Ti(II)–N bonds.[28d,33]

The metrical parameters for the DFT calculated structures of **1** and **2** are given in Table 3. It can be seen that the calculated values are very close to those experimentally measured, an indication that packing forces exert only a minor effect on their core geometries.

Table 4. DFT Calculated UV-Visible Absorption Data for Complexes 1 and 2

calculated (gas phase)		experiment		
λ: nm (eV)	oscillator strength (10^{-2})	λ: nm (eV)	strength (ε, M^{-1} cm^{-1})	λ offset: nm (eV): calc. vs exp.
		$TiCl\{N(H)Ar^{iPr_6}\}_2$ (**1**)		
478(2.59)	3.75	415(2.99)	2700	−0.40
368(3.37)	6.26	356(3.48)	4200	−0.11
286(4.34)	3.68	298(4.16)	11000	0.18
		$Ti\{N(H)Ar^{iPr_6}\}_2$ (**2**)		
451(2.75)	2.75	451(2.75)	2400	0.00
367(3.38)	16.62	363(3.42)	5500	−0.04
282(4.40)	5.47	293(4.23)	10000	0.17

dx.doi.org/10.1021/ic4021355 | *Inorg. Chem.* 2013, 52, 14216–14223

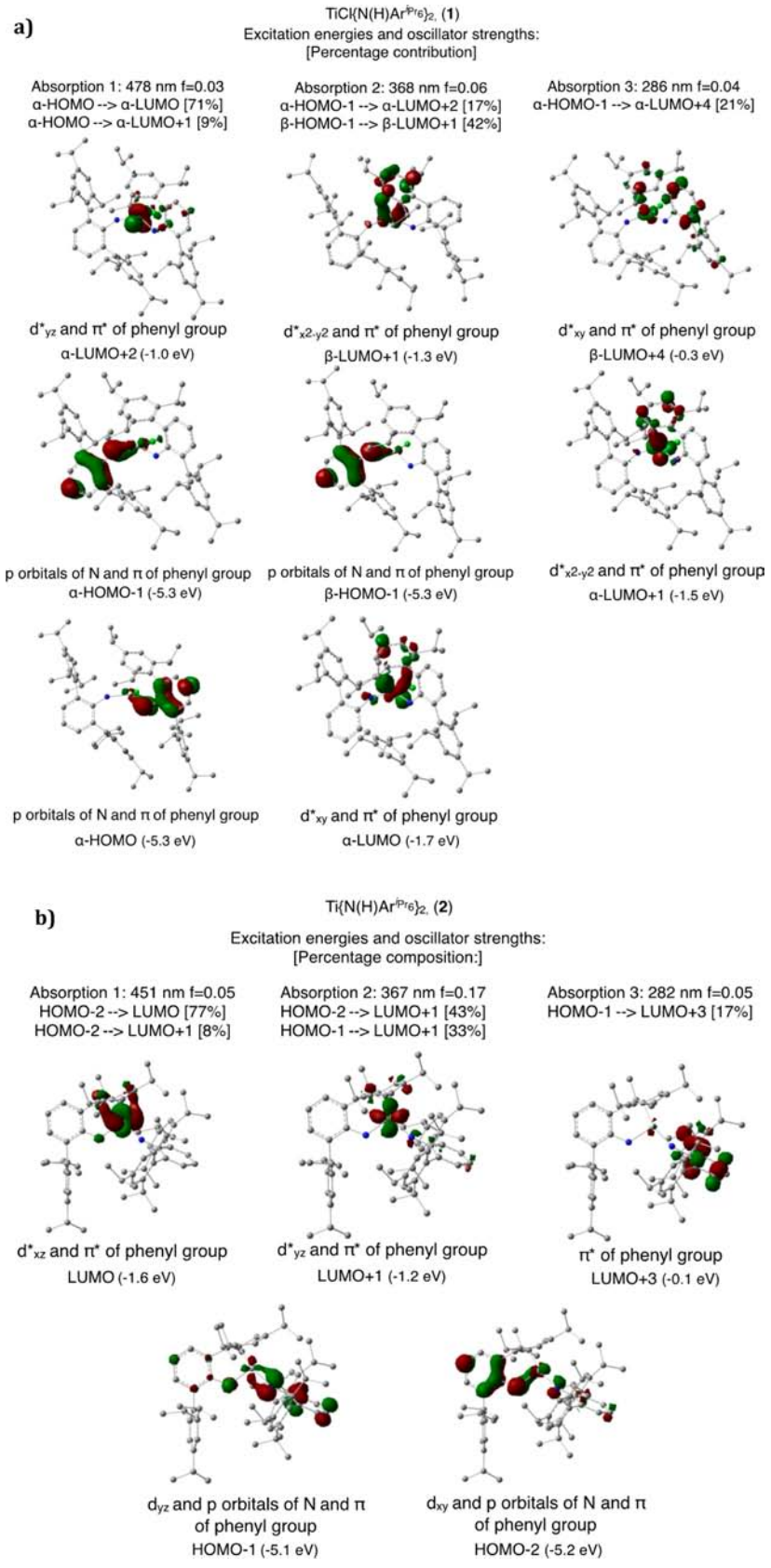

Figure 4. DFT calculated electronic transitions for (a) TiCl{N(H)Ar^{iPr_6}}$_2$ (**1**) and (b) Ti{N(H)Ar^{iPr_6}}$_2$ (**2**).

Electronic Spectroscopy. The UV−visible absorption spectra of the intensely colored orange and orange-brown complexes **1** and **2** in mM hexane solution revealed moderately intense electronic transitions. UV−vis absorption maxima (λ_{max}, nm (ε, M^{-1} cm^{-1})) were observed at 298(11,000), 356(4200), and 415(2700) for complex **1**. Complex **2** displayed absorption

dx.doi.org/10.1021/ic4021355 | *Inorg. Chem.* 2013, 52, 14216−14223

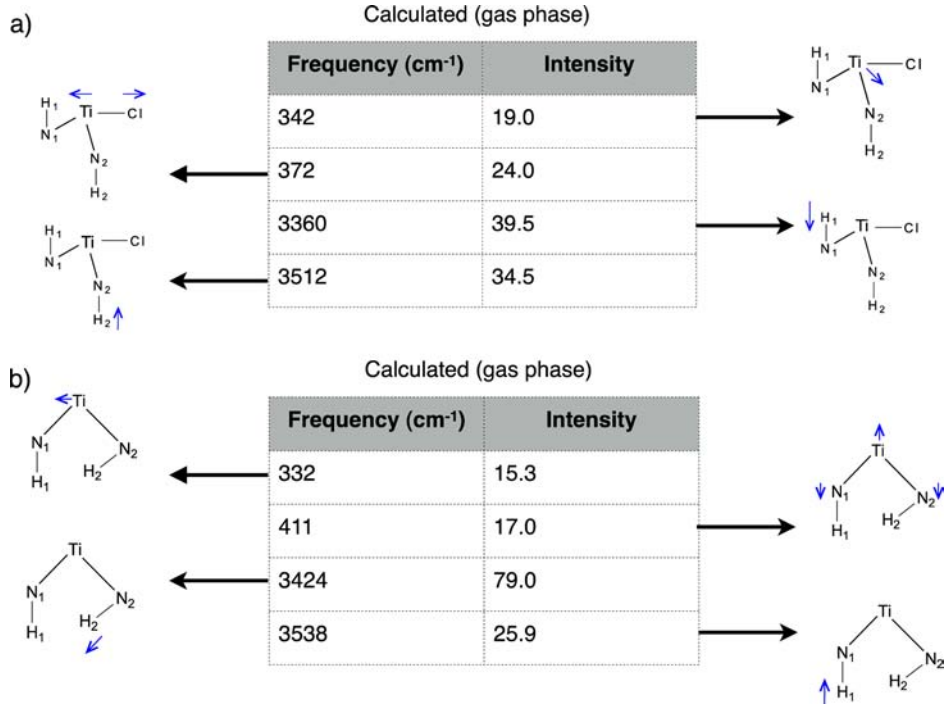

Figure 5. DFT calculated infrared spectra for (a) complex TiCl{N(H)Ar^{iPr_6}}$_2$ (**1**) and (b) complex Ti{N(H)Ar^{iPr_6}}$_2$ (**2**).

maxima (λ_{max}, nm (ε, M^{-1} cm^{-1})) at 293(10000), 363(5500), and 451(2400).

DFT calculations at the B3PW91 level for complex **1** indicated good agreement with the experimentally observed spectroscopic data (Table 4). The highest energy absorption (286 nm, 34965 cm^{-1}) that was calculated (cf. observed values, 298 nm, 11 000 cm^{-1}) corresponds to the ligand to metal electron transfer transition involving p orbitals of N and the π orbitals of the ligand phenyl group (HOMO-1) to π^* of the ligand phenyl group and the d^*_{xy} orbital (LUMO+4) (Table 4). This high-energy absorption is also observed in complex **2** (Table 4). The energy difference between the experimental and the theoretically calculated value is 0.40 eV, or 3226 cm^{-1}. A weaker absorption was calculated to appear at 368 nm, and corresponds to transitions involving the p orbitals of nitrogen and the π orbitals of the ligand phenyl group (HOMO-1) to the d^*_{yz} and the π^* (aryl) ligand orbital (LUMO+2) and p orbitals of nitrogen and π orbital of the ligand phenyl group (HOMO-1) to the π^* of the ligand phenyl group and the empty $d_{x^2-y^2}$ orbital (LUMO+1) (Figure 4a). The weakest absorption is 478 nm or 20921 cm^{-1} in comparison to an observed value at 415 nm. This corresponds to transitions involving the p orbitals of nitrogen and the π orbitals of the ligand phenyl group (HOMO) to the d^*_{xy} and the π^* (aryl) ligand orbital (LUMO) and p orbitals of nitrogen and π orbital of the ligand phenyl group (HOMO) to the π^* of the ligand phenyl group and the $d^*_{x^2-y^2}$ orbital (LUMO+1).

For complex **2**, the three calculated and observed absorption maxima were very similar to those of **1**. The highest energy absorption (282 nm, 35461 cm^{-1}) that was calculated corresponds to the absorption observed at 293 nm from the d_{yz} and the p orbitals of N and the π of the phenyl group (HOMO-1) to the π^* of the phenyl group. The absorption at 367 nm corresponds to a transition from the d_{xy} and the p orbitals of N and the π of the phenyl group (HOMO-2) to the π^* of the ligand phenyl group and the empty d^*_{yz} orbital (LUMO+1) and from the d_{yz} and the p orbitals of N and the π of the phenyl group (HOMO-1) to the π^* of the ligand phenyl group and the empty d^*_{yz} orbital (LUMO+1). The absorption calculated at 451 nm is a transition involving the d_{xy} and p orbitals of nitrogen and the π of the phenyl group orbitals (HOMO-2) to the d^*_{xz} and the π^* of the phenyl group (LUMO) and the d_{xy} and the p orbitals of N and the π of the phenyl group (HOMO-2) to the π^* of the ligand phenyl group and the empty d^*_{yz} orbital (LUMO+1) (Figure 4b). Overall the data in Table 4 represent good agreement between the calculated and experimental spectra.

Infrared Spectroscopy. Infrared spectra for compounds **1** and **2** were recorded as Nujol mulls between CsI plates on a Perkin-Elmer 1430 Infrared spectrometer. Each spectrum displayed two N−H absorptions in the range 3500−3300 cm^{-1} corresponding to the predicted absorption at 3512 and 3360 cm^{-1} (Figure 5a) and 3538 and 3424 cm^{-1} (Figure 5b). The absorption at 342 cm^{-1} for compound **1** (hidden beneath Ti−Cl stretch) and at 411 cm^{-1} (observed at 363 cm^{-1}) for compound **2** can be attributed to a stretching vibration for the N−Ti−N unit on the basis of calculations (Figure 5). The absorption observed at 363 cm^{-1} for compound **1** corresponds to the Ti−Cl stretching vibration calculated at 372 cm^{-1} (Figure 5a). Other predicted absorptions are obscured by ligand and Nujol absorptions and are shown in Supporting Information, Figure SI (2).

Magnetic Properties. The magnetic properties of **2** indicate that above about 50 K its molar magnetic susceptibility, χ_M, is constant at −0.00083(2) emu/mol, a value that indicates that **2** is diamagnetic, in agreement with its formulation as a Ti(IV) species from the structural data. This value is in good agreement with the value of −0.000769 emu/mol obtained from Pascal's constants. Below about 50 K χ_M for **2** begins to increase gradually up to a value of 0.00238 emu/mol at 2 K. This increase is probably the result of the presence of about 0.4 wt % of the paramagnetic titanium(III) starting material, **1**. At 5 K in an applied field of 7 T the molar magnetization of **2** is 0.0064 Nβ, a

dx.doi.org/10.1021/ic4021355 | Inorg. Chem. 2013, 52, 14216−14223

very small value that is consistent with the presence of the above-mentioned trace of titanium(III) starting material.

The magnetic properties of **1** are indicative of a paramagnetic titanium(III) complex in the presence of spin−orbit coupling. A fit of $\chi_M T$ obtained between 5 and 300 K with the expression,

$$\chi_M T = \left(1 - \frac{4\lambda}{10Dq}\right)\frac{CT}{(T-\theta)} + N\alpha T$$

is shown in Figure 6. In these fits there would be a perfect correlation between the Curie constant, C, and $4\lambda/10Dq$ and, as a consequence, C has been fixed to 0.3751 emu K/mol, the value that corresponds to the spin-only moment of 1.732 μ_B of titanium(III) with $S = 1/2$ and $g = 2$. Thus the fit has been obtained by adjusting the Weiss temperature, q, the second order Zeeman contribution to the molar susceptibility, $N\alpha$, and $4\lambda/10Dq$, which accounts for the spin−orbit coupling of the titanium(III) ion,[34,35] where λ is the titanium(III) spin−orbit coupling constant and $10Dq$ is the crystal-field experienced by the pseudotetrahedral titanium(III) ion. The resulting fit is excellent and, if one assumes that the complex is unsolvated, yields $q = 0.15(3)$ K, $N\alpha = 0.000809(3)$ emu/mol, and $4\lambda/10Dq = 0.608(1)$ with a fixed value of $C = 0.3751$ emu K/mol. If one assumes the free-ion titanium(III) spin−orbit coupling constant $\lambda = 155$ cm^{-1} is valid, the corresponding crystal field is $10Dq = 1020(2)$ cm^{-1} which is similar to those in other three-coordinate compounds.[36]

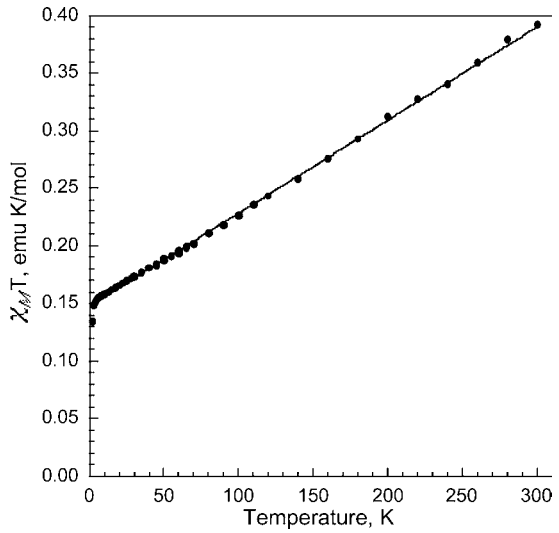

Figure 6. Temperature dependence of $\chi_M T$ measured for unsolvated **2** upon warming from 2 to 300 K in an applied field of 0.01 T and fit between 5 and 300 K by assuming the presence of titanium(III) spin−orbit coupling.

The corresponding fit for **1** obtained by assuming that the sample is fully solvated as is observed in the X-ray structure discussed above, is shown in the Supporting Information, Figure SI(3a). In this case the fit yields $q = 0.14(3)$ K, $N\alpha = 0.000941(4)$ emu/mol, and $4\lambda/10Dq = 0.546(1)$ with a fixed value of $C = 0.3751$ emu K/mol. If one assumes the free-ion titanium(III) spin−orbit coupling constant $\lambda = 155$ cm^{-1} is valid, the corresponding crystal field is $10Dq = 1135(2)$ cm^{-1}. It is quite difficult to determine the extent to which **1** has lost its solvation molecules during the process of measuring its magnetic susceptibility, and the true parameters may lie between the two limiting cases presented above.

The magnetization of **1** measured at 5 K, see Supporting Information, Figure SI(3b), increases in a slightly nonlinear fashion from 0 to 0.290 Nβ as the field increases from 0 to 7 T and is far from saturation even at 7 T. The slope of the magnetization measured between 0 and 5000 Oe is linear with a slope of 0.0302 emu/mol, a value that yields a μ_{eff} of 1.10 μ_B, values that agree rather well with the $\chi_M = 0.03545$ emu/mol and $\mu_{eff} = 1.19$ μ_B observed at 5 K and 0.01 T.

CONCLUSIONS

In conclusion, we have synthesized and characterized the new titanium complexes TiCl{N(H)Ar^{iPr_6}}$_2$ (**1**) and Ti{N(H)Ar^{iPr_6}}$_2$ (**2**). The reduction of **1** with potassium graphite afforded **2** which, unlike its other first row transition metal analogues M(N(H)Ar^{iPr_6}}$_2$ (M = V, Cr, Mn, Fe, Co, and Ni), does not have two-coordinate geometry. Instead titanium undergoes a cyclization reaction with one of the flanking aryl rings of a −{N(H)Ar^{iPr_6}} ligand to yield a product that is a four-coordinate Ti(IV) complex. This apparently occurs because of the larger size of titanium and lower number of valence electrons in comparison to the later metals. Work to synthesize two-coordinate titanium complexes stabilized by bulky ligands less prone to reactions that increase the metal coordination number is in hand.

ASSOCIATED CONTENT

Supporting Information

CIF files for the X-ray structures of **1** and **2** along with additional NMR spectra, IR spectra, magnetic measurements, and a reference. This material is available free of charge via the Internet at http://pubs.acs.org.

AUTHOR INFORMATION

Corresponding Author

*E-mail: pppower@ucdavis.edu.

Notes

The authors declare no competing financial interest.

ACKNOWLEDGMENTS

We thank the National Science Foundation (CHE-1263760) for financial support and (Grant 0840444) for the Dual source X-ray diffractometer. We also thank Peter Klavins for assistance in the magnetization measurements.

REFERENCES

(1) Power, P. P. *Chem. Rev.* **2012**, *112*, 3482.
(2) Kays, D. L. *Dalton Trans.* **2011**, *40*, 769.
(3) Reiff, W. M.; LaPointe, A. M.; Witten, E. H. *J. Am. Chem. Soc.* **2004**, *126*, 10206.
(4) Reiff, W. M.; Schulz, C. E.; Whangbo, M. H.; Seo, J. I.; Lee, Y. S.; Potratz, G. R.; Spicer, C. W.; Girolami, G. S. *J. Am. Chem. Soc.* **2009**, *131*, 404.
(5) Merrill, W. A.; Stich, T. A.; Brynda, M.; Yeagle, G. J.; Fettinger, J. C.; De Hont, R.; Reiff, W. M.; Schulz, C. E.; Britt, R. D.; Power, P. P. *J. Am. Chem. Soc.* **2009**, *131*, 12693.
(6) Bryan, A. M.; Merrill, W. A.; Reiff, W. M.; Fettinger, J. C.; Power, P. P. *Inorg. Chem.* **2012**, *51*, 3366.
(7) Boynton, J. N.; Merrill, W. A.; Reiff, W. M.; Fettinger, J. C.; Power, P. P. *Inorg. Chem.* **2012**, *51*, 3212.
(8) Zadrozny, J. M.; Atanasov, M.; Bryan, A. M.; Lin, C. Y.; Rekken, B. D.; Power, P. P.; Neese, F.; Long, J. R. *Chem. Sci.* **2013**, *4*, 125.
(9) Atanasov, M.; Zadrozny, J. M.; Long, J. R.; Neese, F. *Chem. Sci.* **2013**, *4*, 139.
(10) Zadrozny, J. M.; Xiao, D. J.; Atanasov, M.; Long, G. J.; Grandjean, F.; Neese, F.; Long, J. R. *Nat. Chem.* **2013**, *5*, 577.

(11) (a) Buttrus, N. H.; Eaborn, C.; Hitchcock, P. B.; Sullivan, A. C. *J. Chem. Soc., Chem. Commun.* **1985**, 1380. (b) Viefhaus, T.; Schwartz, W.; Hübler, K.; Locke, K.; Weidlein, J. *J. Anorg. Allg. Chem.* **2001**, *627*, 725. (c) Nguyen, T.; Panda, A.; Olmstead, M. M.; Richards, A. F.; Stender, M.; Brynda, M.; Power, P. P. *J. Am. Chem. Soc.* **2005**, *127*, 8545. (d) Li, J.; Song, H.; Cui, C.; Cheng, J. P. *Inorg. Chem.* **2008**, *47*, 3468. (e) Laskowski, C. A.; Hillhouse, G. L. *J. Am. Chem. Soc.* **2008**, *130*, 13846. (f) Lipschutz, M. I.; Tilley, T. D. *Chem. Commun.* **2012**, *48*, 7146.
(12) Boynton, J. N.; Guo, J.-D.; Fettinger, J. C.; Melton, C. E.; Nagase, S.; Power, P. P. *J. Am. Chem. Soc.* **2013**, *135*, 10720.
(13) Pangborn, A. B.; Giardello, M. A.; Grubbs, R. H.; Rosen, R. K.; Timmers, F. J. *Organometallics* **1996**, *15*, 1518.
(14) Twamley, B.; Hwang, C. S.; Hardman, N. J.; Power, P. P. *J. Organomet. Chem.* **2000**, *609*, 152.
(15) (a) Fredenhagen, K.; Cadenbach, G. *Z. Anorg. Chem.* **1926**, *158*, 249. (b) Bergbreiter, D. E.; Killough, J. M. *J. Am. Chem. Soc.* **1978**, *100*, 2126.
(16) Bradley, D. C.; Copperthwaite, R. G. *Inorg. Synth.* **1978**, *18*, 116.
(17) Hope, H. *Prog. Inorg. Chem.* **1995**, *41*, 1.
(18) (a) Sheldrick, G. M. *SADABS*; Universität Göttingen: Göttingen, Germany, 2008. (b) Sheldrick, G. M. *SHELXTL*, 6.1; Siemens Analytical X-ray Instruments Inc.: Madison, WI, 2002.
(19) Bain, G. A.; Berry, J. F. *J. Chem. Educ.* **2008**, *85*, 532.
(20) Frisch, M. J. *Gaussian 09*, Revision A.01; Gaussian, Inc.: Wallingford, CT, 2009.
(21) (a) Becke, A. D. *J. Chem. Phys.* **1993**, *98*, 1372. (b) Perdew, J. P.; Wang, Y. *Phys. Rev. B* **1992**, *45*, 13244.
(22) Bradley, D. C.; Copperthwaite, R. G. *Inorg. Synth.* **1978**, *18*, 112.
(23) Jones, N. A.; Liddle, S. T.; Wilson, C.; Arnold, P. L. *Organometallics* **2007**, *26*, 755.
(24) Smith, S. B.; Stephan, D. W. *Comprehensive Coordination Chemistry II*; Elsevier: Amsterdam, The Netherlands, 2004; Vol. *4.2*.
(25) (a) Troyanov, S. I.; Antropiusova, H.; Mach, K. *J. Organomet. Chem.* **1992**, *427*, 49. (b) Calderazzo, F.; Pampaloni, G.; Tripepi, G. *Organometallics* **1997**, *16*, 4943.
(26) Cuenca, T. *Comprehensive Organometallic Chemistry II*; Elsevier: Amsterdam, The Netherlands, 2007; Vol. *4.05*.
(27) (a) Pyykko, P.; Atsumi, M. *Chem.—Eur. J.* **2009**, *15*, 186. (b) Pyykko, P.; Atsumi, M. *Chem.—Eur. J.* **2009**, *15*, 12770. (c) Shannon, R. D.; Prewitt, C. T. *Acta Crystallogr.* **1969**, *B25*, 925.
(28) (a) Lappert, M.; Protchenko, A.; Power, P. P.; Seeber, A. *Metal Amide Chemistry*; John Wiley & Sons: Chichester, U.K., 2008; p 370; (b) Scoles, L.; Gambarotta, S. *Inorg. Chim. Acta* **1995**, *235*, 375. (c) Fickes, M. G.; Davis, W. M.; Cummins, C. C. *J. Am. Chem. Soc.* **1995**, *117*, 6384. (d) Beydoun, N.; Duchateau, R.; Gambarotta, S. *J. Chem. Soc., Chem. Commun.* **1992**, 244. (e) Putzer, M. A.; Magull, J.; Goesmann, H.; Neumüller, B.; Dehnicke, K. *Chem. Ber.* **1996**, *129*, 1401.
(29) Ni, C. B.; Rekken, B.; Fettinger, J. C.; Long, G. J.; Power, P. P. *Dalton Trans.* **2009**, 8349.
(30) March, J. *Advanced Organic Chemistry*, 4th ed.; Wiley: New York, 1992; p 21.
(31) Hagadorn, J. R.; Arnold, J. *Angew. Chem., Int. Ed.* **1998**, *37*, 1729.
(32) Graham, T. W.; Kickham, J.; Courtenay, S.; Wei, P.; Stephan, D. W. *Organometallics* **2004**, *23*, 3309.
(33) Duchateau, R.; Gambarotta, S.; Beydoun, N.; Bensimon, C. *J. Am. Chem. Soc.* **1991**, *113*, 8986.
(34) Figgis, B. N. *Introduction to Ligand Fields*; Wiley-Interscience: New York, 1966.
(35) Kahn, O. *Molecular Magnetism*; VCH Publishers: New York, 1993.
(36) (a) Alyea, E. C.; Bradley, D. C.; Copperthwaite, R. G.; Sales, K. D. *Dalton Trans.* **1973**, *2*, 185. (b) Eller, P. G.; Bradley, D. C.; Hursthouse, M. B.; Meek, D. W. *Coord. Chem. Rev.* **1977**, *24*, 1. (c) Cummins, C. C. *Prog. Inorg. Chem.* **1998**, *47*, 885. (d) Alvarez, S. *Coord. Chem. Rev.* **1999**, *193-5*, 13. (e) Krishnamurthy, R.; Schaap, W. B. *J. Chem. Educ.* **1969**, *46*, 799. (f) Bryan, A. M.; Long, G. J.; Grandjean, F.; Power, P. P. *Inorg. Chem.* **2013**, *52*, 12152.